Fresh look at the diffuse ALP background from supernovae

Francisco R. Candón[1,*], Sougata Ganguly[2,†], Maurizio Giannotti[1,3,‡]
Tanmoy Kumar[4,§], Alessandro Lella[5,6,‖] and Federico Mescia[7,¶]

[1]*Centro de Astropartículas y Física de Altas Energías, University of Zaragoza,*
Zaragoza, 50009, Aragón, Spain
[2]*Particle Theory and Cosmology Group, Center for Theoretical Physics of the Universe,*
Institute for Basic Science (IBS), Daejeon, 34126, Korea
[3]*Physical Sciences, Barry University, 11300 NE 2nd Avenue, Miami Shores, Florida 33161, USA*
[4]*School of Physical Sciences, Indian Association for the Cultivation of Science,*
2A & 2B Raja S.C. Mullick Road, Jadavpur, Kolkata 700032, India
[5]*Dipartimento Interateneo di Fisica "Michelangelo Merlin," Via Amendola 173, 70126 Bari, Italy*
[6]*Istituto Nazionale di Fisica Nucleare-Sezione di Bari, Via Orabona 4, 70126 Bari, Italy*
[7]*Istituto Nazionale di Fisica Nucleare, Laboratori Nazionali di Frascati, C.P. 13, 00044 Frascati, Italy*

Protoneutron stars, highly compact objects formed in the core of exploding supernovae (SNe), are powerful sources of axionlike particles (ALPs). In the SN core, ALPs are dominantly produced via nucleon-nucleon bremsstrahlung and pion conversion, resulting in an energetic ALP spectrum peaked at energies $\mathcal{O}(100)$ MeV. In this work, we revisit the diffuse ALP background, produced from all past core-collapse supernovae, and update the constraints derived from *Fermi*-LAT observations. Assuming the maximum ALP-nucleon coupling allowed by the SN 1987A cooling, we set the upper limit $g_{a\gamma\gamma} \lesssim 2 \times 10^{-13}$ GeV^{-1} for ALP mass $m_a \lesssim 10^{-10}$ eV, which is approximately a factor of two improvement with respect to the existing bounds. On the other hand, for $m_a \gtrsim 10^{-10}$ eV, we find that including pion conversion strengthens the bound on $g_{a\gamma\gamma}$, approximately by a factor of two compared to the constraint obtained from bremsstrahlung alone. Additionally, we present a sensitivity study for future experiments such as AMEGO-X, e-ASTROGAM, GRAMS-balloon, GRAMS-satellite, and MAST. We find that the expected constraint from MAST would be comparable to *Fermi*-LAT bound. However, SN 1987A constraint remains one order of magnitude stronger as compared to the bound derived from the current and future gamma-ray telescopes.

I. INTRODUCTION

The core collapse of massive stars leads to the formation of a protoneutron star (PNS), a hot and dense astrophysical environment capable of producing axionlike particles (ALPs). Core-collapse supernovae (SNe) may act as cosmic factories of axions and axionlike particles (ALPs) [1–4], providing an opportunity to probe these particles and their couplings using a variety of techniques.

These weakly interacting pseudoscalar particles, if sufficiently light, can be abundantly produced and escape the PNS, contributing to a diffuse background of SN ALPs, analogous to the diffuse supernova neutrino background. Historically, supernovae have played a crucial role in constraining ALP properties, particularly following the detection of the SN 1987A neutrino burst. Indeed, the SN 1987A neutrino detection was a milestone event for axion physics (see Refs. [5,6] for recent reviews).

The axion emission leads to an additional energy loss, which could, in principle, have an observable impact on the detected neutrino signal. This argument led to very stringent limits on the ALP-nucleon interactions. Primarily, the focus has been on the nucleon-nucleon (NN) bremsstrahlung process [7–16] as the dominant production mechanism. However, more recently, the ALP production from negatively charged pions via $\pi^- + p \rightarrow a + n$, has emerged as the potentially dominant process [17–21].

[*]Contact author: francandon@unizar.es
[†]Contact author: sganguly0205@ibs.re.kr
[‡]Contact author: mgiannotti@unizar.es
[§]Contact author: kumartanmoy1998@gmail.com
[‖]Contact author: alessandro.lella@ba.infn.it
[¶]Contact author: federico.mescia@lnf.infn.it

If ALPs interact exclusively with photons, their production in supernovae occurs through the Primakoff process. However, this mechanism is relatively inefficient, making the resulting cooling bound less competitive compared to constraints from globular clusters [22–24] (which are applicable for ALP masses $\lesssim 50$ keV [25–27]). Nonetheless, light ALPs produced in SNe can convert into gamma rays while traversing through the magnetic field of the Milky Way [28,29]. The absence of a gamma-ray signal coincident with the SN 1987A neutrino burst in the data from the Gamma-Ray Spectrometer (GRS) aboard the Solar Maximum Mission (SMM) led to stringent constraints on the ALP-photon coupling [28,29]. In particular, the most recent analysis performed for ALPs coupling only to photons reports an upper bound on $g_{a\gamma\gamma} < 5.3 \times 10^{-12}$ GeV^{-1} for $m_a < 4 \times 10^{-10}$ eV [30] (see also the revision in [31]).

Future Galactic supernovae occurring during the operational lifetime of the Large Area Telescope aboard the *Fermi* satellite (*Fermi*-LAT) could significantly enhance these constraints [32–34]. The sensitivity to light ALPs converting into gamma rays in the Galactic magnetic field would be further improved if ALPs also couple to nucleons, as nucleon-induced processes can boost the ALP production rate [35]. Additionally, the detection of a gamma-ray signal in *Fermi*-LAT would provide valuable insights into the SN explosion mechanism, allowing one to probe the properties of the SN core and assess the relevance of the pion-induced production channel for ALPs. Ultimately, this could shed light on the equation of state of dense nuclear matter [35].[1]

Finally, Ref. [43] adopted a significantly different approach and investigated the diffuse ALP flux originating from past core-collapse SNe. The study showed that the cumulative emission of ALPs from all past core-collapse events gives rise to a diffuse flux with characteristic energies of $\mathcal{O}(50)$ MeV. The nondetection of a diffuse supernova ALP background (DSALPB) was used to constrain ALP couplings to photons and nucleons, leveraging measurements of the diffuse gamma-ray flux obtained by the *Fermi*-LAT telescope. As expected, the inclusion of ALP-nucleon interactions significantly enhances the ALP production rate in SNe via the nucleon-nucleon bremsstrahlung process. Assuming the largest phenomenologically allowed ALP-nucleon coupling, the upper bound $g_{a\gamma\gamma} \lesssim 6 \times 10^{-13}$ GeV^{-1} for $m_a \lesssim 10^{-11}$ eV was derived.[2]

In this work, we revisit the analysis presented in Ref. [43] by incorporating key improvements that refine
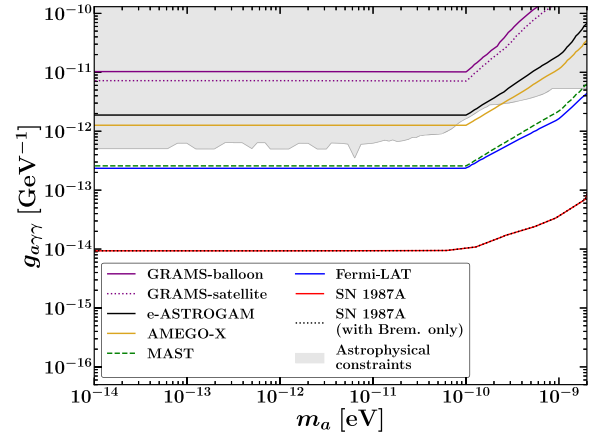

FIG. 1. Projected constraints in the $m_a - g_{a\gamma\gamma}$ plane from future gamma ray missions AMEGO-X [45], e-ASTROGAM [46], GRAMS-balloon [47], GRAMS-satellite [47], and MAST [48]. Here we have considered supernova ALP production via both bremsstrahlung and pion conversion. For deriving the above constraints, we have assumed $g_{ap} = 5 \times 10^{-10}$ and $g_{an} = 0$. The constraint from *Fermi*-LAT is shown by the blue solid line. The solid red line denotes the SN 1987A constraint considering both bremsstrahlung and pion conversion, whereas the case of ALP production only via bremsstrahlung is shown with the black dotted line. The gray shaded region represents combined astrophysical constraint on $g_{a\gamma\gamma}$ considering ALPs not to be a dark matter candidate [49].

the constraints on the DSALPB. First, we account for the additional ALP production via the pion-induced process, which is now recognized as the dominant production mechanism in supernovae. This represents a significant advancement over previous studies, as it modifies both the expected ALP flux and its spectral distribution. As expected, the inclusion of the pion-induced production channel significantly alters the expected DSALPB spectrum, leading to a spectral hardening, as illustrated in Fig. 2. In particular, the peak energy shifts to $\gtrsim 100$ MeV, modifying both theoretical expectations and the experimental requirements for detection.

Second, we assess the sensitivity of future (proposed) observational campaigns to detect the DSALPB signal. Our results are summarized in Fig. 1. As we shall show, and as evident from Fig. 1, *only* MAST would have the required sensitivity to be competitive with *Fermi*-LAT. Hence, it is unlikely that any of the future telescopes, in their currently proposed configurations, would be able to make a breakthrough in DSALPB searches. We believe that this is an additional motivation for the next-generation MeV-range missions, which could search for the DSALPB and explore previously inaccessible regions of ALP parameter space and significantly enhance the prospects for discovery.

The paper is organized as follows: In Sec. II, we introduce the effective Lagrangian governing ALP interactions. In Sec. III, we describe the production mechanisms

---

[1]The direct detection of SN ALPs from Earth, which do not rely on the conversion in the galactic magnetic field, has also been explored in a series of recent studies [36–42].

[2]Constraints on $g_{a\gamma\gamma}$ at higher ALP masses, incorporating the pionic contribution, from the nonobservation of the DSALPB by *Fermi*-LAT have been discussed in Ref. [44].

in supernovae for ALPs coupled to nuclear matter and compute the resulting DSALPB flux. Section IV discusses ALP-photon conversion in the Milky Way's magnetic field and the expected gamma-ray signal. Finally, in Sec. V, we present our results on the projected constraints on ALP couplings from future observations and conclude in Sec. VI.

II. EFFECTIVE LAGRANGIAN OF ALP

The phenomenological ALP Lagrangian relevant for our study can be written as

$$\mathcal{L}_a = \frac{1}{2}\partial_\mu a \partial^\mu a - \frac{1}{2}m_a^2 a^2 - \frac{g_{a\gamma\gamma}}{4}a F_{\mu\nu}\tilde{F}^{\mu\nu} + \mathcal{L}_{\text{nuc}}, \quad (1)$$

where m_a is the mass of the ALP and $g_{a\gamma\gamma}$ is the coupling of the ALP with the photon. The last term $\mathcal{L}_{\text{nuc}}$ contains the interaction of ALP with hadrons as well as other hadronic interaction vertices relevant for ALP production processes. Additional possible interaction terms, for example with electrons and positrons, will be ignored in this study. The explicit form of $\mathcal{L}_{\text{nuc}}$ is given by [16,19,50]

$$\begin{aligned}\mathcal{L}_{\text{nuc}} = \frac{\partial^\mu a}{2m_N}&[g_{ap}\bar{p}\gamma_\mu\gamma_5 p + g_{an}\bar{n}\gamma_\mu\gamma_5 n \\ &+ \frac{g_{a\pi N}}{f_\pi}(i\pi^+\bar{p}\gamma_\mu n - i\pi^-\bar{n}\gamma_\mu p) \\ &+ g_{aN\Delta}(\bar{p}\Delta_\mu^+ + \bar{\Delta}_\mu^+ p + \bar{n}\Delta_\mu^0 + \bar{\Delta}_\mu^0 n)] \\ &+ \frac{g_A}{2f_\pi}[\partial_\mu\pi^0(\bar{p}\gamma^\mu\gamma_5 p - \bar{n}\gamma^\mu\gamma_5 n) \\ &+ \sqrt{2}\partial_\mu\pi^+\bar{p}\gamma^\mu\gamma_5 n + \sqrt{2}\partial_\mu\pi^-\bar{n}\gamma^\mu\gamma_5 p],\end{aligned} \quad (2)$$

where nucleon mass $m_N = 0.938$ GeV, $g_A = 1.28$, and the pion decay constant $f_\pi = 92.4$ MeV. The first two terms are the trilinear interactions of ALP with proton and neutron with coupling coefficients g_{ap} and g_{an}, respectively. The four-particle interaction terms among ALP, pion, neutron, and proton are given in the second line of Eq. (2) with coupling coefficient $g_{a\pi N} = (g_{ap} - g_{an})/\sqrt{2}g_A$ [16] whereas ALP-Δ baryons interactions are written in the third line and $g_{aN\Delta} = -\sqrt{3}/2(g_{ap} - g_{an})$ [20]. The relevant interactions between pion and nucleons in the context of SN physics are described in the last two lines of Eq. (2).

In Eq. (2), the interaction terms between the ALP and neutrons, protons, and negatively charged pions facilitate ALP production from the nuclear plasma within the PNS, as discussed in Ref. [21]. In the next section, we briefly review the production of ALP from a PNS.

III. ALP PRODUCTION FROM PNS

In the presence of ALP-nucleon interactions, ALPs can be copiously produced from the hot and dense environment

of a PNS, primarily via *NN*-bremsstrahlung and pion conversion.[3]

The rate of ALP production via *NN*-bremsstrahlung per unit volume and per unit ALP energy interval can be calculated as [6]

$$\begin{aligned}\left(\frac{d^2 n_a}{dE_a dt}\right)_{NN} = \frac{p_a}{4\pi^2}\int &\left[\prod_{i=1}^4 d\Pi_i\right] \\ &\times (2\pi)^4\delta^4(P_1 + P_2 - P_3 - P_4 - P_a) \\ &\times S|\mathcal{M}|_{NN}^2 f_1 f_2(1 - f_3)(1 - f_4),\end{aligned} \quad (3)$$

where the four momenta of initial and final state nucleons are $P_i = (E_i, \vec{p}_i)$ with $(i = 1, ..., 4)$. $P_a = (E_a, \vec{p}_a)$ is the four momentum of ALP and $p_a \equiv |\vec{p}_a|$. $d\Pi_i = d^3\vec{p}_i/(2\pi)^3 2 E_i$ is the Lorentz invariant phase space measure, $|\mathcal{M}|_{NN}^2$ is the matrix amplitude square of the bremsstrahlung process, summed over initial and final spins, and S is the symmetry factor for the identical particles in the initial and final states. f_i $(i = 1, ..., 4)$ are the energy distribution functions of the initial and final state nucleons and their explicit form is

$$f_i(E_i) = \left[\exp\left(\frac{E_i - \mu_i}{T_{SN}}\right) + 1\right]^{-1}, \quad (4)$$

where T_{SN} is the temperature of the PNS and μ_i is the chemical potential. Inside the PNS, $T_{\text{SN}} \sim 30$ MeV and thus protons and neutrons are nonrelativistic. Assuming negligible recoil momenta of the nucleons, the magnitude of their 3-momentum is $\sim\sqrt{m_N T_{SN}} \approx 168$ MeV, whereas for $T_{SN} \gg m_a$, $p_a \sim T_{SN}$. Since $p_a \ll |\vec{p}_i|$, we neglect $\vec{p}_a$ with respect to $\vec{p}_i$ in the momentum conservation condition in Eq. (3) [14,16,51].

ALPs can also be produced from negatively charged pions via $\pi^- + p \to n + a$ process. We can write the ALP production rate per unit volume and per unit ALP energy interval as [6]

$$\begin{aligned}\left(\frac{d^2 n_a}{dE_a dt}\right)_{\pi N} = \frac{p_a}{4\pi^2}\int &d\Pi_\pi d\Pi_n d\Pi_p \\ &\times (2\pi)^4 \times \delta^4(P_p + P_\pi - P_n - P_a) \\ &\times |\mathcal{M}|_{\pi N}^2 f_\pi f_p(1 - f_n),\end{aligned} \quad (5)$$

where P_n, P_p, and P_π are the four momentum of neutron, proton, and pion respectively. The energy distribution functions of protons and neutrons are denoted by f_p and f_n, respectively, and their analytical form is given in

---

[3]In the SN core, ALPs can also be produced via Primakoff process [43]. However, the ALP flux from the Primakoff process is noncompetitive with respect to the bremsstrahlung and pion conversion processes for the values of $g_{a\gamma\gamma}$ allowed by other bounds.

Eq. (4). The energy distribution function of negatively charged pions is

$$f_\pi = \left[\exp\left(\frac{E_\pi - \mu_\pi}{T_{SN}}\right) - 1\right]^{-1}, \tag{6}$$

where μ_π is the chemical potential of the negatively charged pions inside the PNS and it is calculated using the β-equilibrium condition, $\mu_\pi = \mu_n - \mu_p$ [52]. Finally $|\mathcal{M}|^2_{\pi N}$ is the matrix amplitude square of $\pi^- + p \to n + a$, summed over initial and final state spins. Since nucleons are non-relativistic in SN environment, we approximated $E_n \sim E_p$ in the calculation of ALP production rate from pion conversion, so that $E_a \simeq E_\pi$ where E_π is the energy of negatively charged pion. Hence the total production rate of ALPs inside a newly born PNS per unit volume and per unit ALP energy interval is the sum of the above two contributions

$$\left(\frac{d^2 n_a}{dE_a dt}\right)_{\text{total}} = \left(\frac{d^2 n_a}{dE_a dt}\right)_{NN} + \left(\frac{d^2 n_a}{dE_a dt}\right)_{\pi N}. \tag{7}$$

Once produced, ALPs with sufficiently high kinetic energies can escape the PNS provided that the ALP-nucleon coupling is not very large such that the scattering rate of ALPs with the nucleons in the PNS medium is small. This regime is known as *free-streaming regime*. Reference [21] pointed out that ALPs with nuclear couplings $g_{aN} \lesssim 10^{-8}$ would stream out from the SN core without relevant absorption effects. While traveling out of the PNS, the produced ALPs have to overcome the strong gravitational potential generated in the densest regions of the PNS. As a result, their energy spectrum gets red-shifted, i.e., an ALP that is produced inside the PNS with energy E_a, after escaping the PNS, is left with an energy E_a^* where

$$E_a^* = \alpha(r) E_a, \tag{8}$$

with $\alpha(r)$ being the lapse factor that encodes the red-shifting of the energy in the gravitational potential of the PNS. The values of α and other SN parameters such as density, temperature, and chemical potential at each radius are obtained from the SN simulation model SFHo-s18.8 with progenitor mass $18.8 M_\odot$ by the GARCHING group [53], which was also previously used in [19,21,35,41,54]. As discussed in [41], in this model, the highest temperature (~ 40 MeV) is achieved during the early cooling phase i.e., between $t = 1$–2 s after which it decreases. The core density, on the other hand, increases from 6×10^{14} gm/cm^3 at $t = 1$ s to 8×10^{14} gm/cm^3 at $t = 6$ s. The abundance of the negatively charged pions, which strongly depends on the SN temperature, reaches its

maximum value ($\sim \mathcal{O}(1\%)$ of the nucleon abundance) during the early cooling phase and at the later stage of cooling it is negligible.

Following [19], the spectra of ALPs produced from a single core collapse SN, taking into account the gravitational redshift, is then given by

$$\frac{dN_a}{dE_a} = \int d^3\vec{r} \int dt^* \alpha(r) \left(\frac{d^2 n_a^*}{dE_a^* dt^*}\right)_{\text{total}}. \tag{9}$$

Before ending this section, let us stress the following points: (i) as benchmark values for ALP-nucleon couplings, we consider $g_{an} = 0$ and $g_{ap} \neq 0$, as in KSVZ model [55], and (ii) we are interested in the free-streaming regime of ALP where the absorption of ALP via inverse bremsstrahlung, $a + n(p) \to p(n) + \pi^-(\pi^+)$, and $a + n(p) \to n(p) + \pi^0$ is negligible. Therefore we do not consider ALP absorption while calculating the ALP flux.

A. Diffuse ALP background

As discussed in the previous sections, ultralight ALPs produced from the core-collapse supernovae over the entire history of our Universe give rise to a homogeneous and isotropic DSALPB [43,56]. If ALPs are produced primarily by pionic processes, the DSALPB spectrum peaks at energies $E \sim \mathcal{O}(100 \text{ MeV})$.

According to Ref. [43], the DSALPB flux is given by

$$\frac{d\phi_a}{dE_a} = \int_0^\infty (1+z) \frac{dN_a(E_a(1+z))}{dE_a} R_{\text{SN}}(z) \left(\left|\frac{dt}{dz}\right|\right) dz, \tag{10}$$

where z is the redshift, $R_{\text{SN}}(z)$ is the SN explosion rate, taken from Ref. [57], with a total normalization for the core-collapse rate $R_{cc} = 1.25 \times 10^{-4}$ yr^{-1} Mpc^{-3}. Furthermore, $|dt/dz|^{-1} = H_0(1+z)[\Omega_\Lambda + \Omega_m(1+z)^3]^{1/2}$ with the cosmological parameters $H_0 = 67.4$ km s^{-1} Mpc^{-1}, $\Omega_m = 0.315$, and $\Omega_\Lambda = 0.685$.

In Fig. 2, we show the flux of diffuse supernova ALPs, $E_a^2 d\phi_a/dE_a$, from all past core collapse supernovae. For this figure, we are assuming $g_{ap} = 5 \times 10^{-10}$, a value allowed by the SN 1987A cooling constraint, as discussed in [21]. We explicitly show the contribution of the ALP flux from NN-bremsstrahlung (red dashed line) and pion conversion (red dotted line) as well as the total flux (red solid line). We remark that, while NN-bremsstrahlung represents the primary contribution to the DSALPB flux in the low energy regime $E_a \lesssim 100$ MeV, the high-energy component of the spectrum is dominated by ALPs produced via pionic processes.
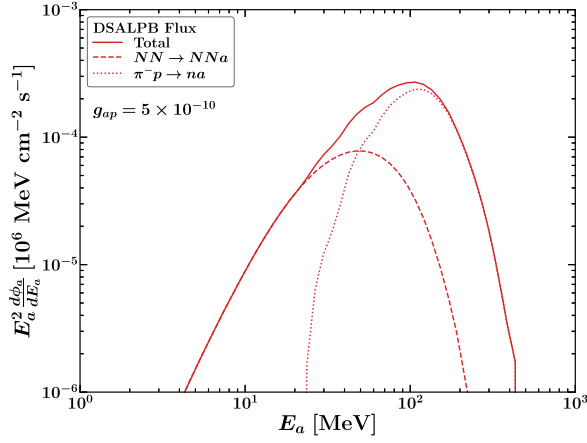
FIG. 2. DSALPB flux arising due to the contribution of all past core collapse supernovae. We assume $g_{ap} = 5 \times 10^{-10}$ which is below the cooling bound [21]. The total DSALPB flux, considering ALP production via both NN-bremsstrahlung and pion conversion in the PNS, is shown by the red solid line. The red dashed line and the red dotted line are the DSALPB fluxes considering only the NN-bremsstrahlung and the pion conversion process respectively.

IV. GAMMA RAYS FROM DSALPB CONVERSION IN GALACTIC MAGNETIC FIELD

As ALPs from the DSALPB travel toward Earth, they traverse the Milky Way's magnetic field, where their coupling $g_{a\gamma\gamma}$ can induce oscillations into photons [58].[4]

To calculate the final gamma-ray flux arising from ALP photon oscillation, we need to consider the exact structure of the galactic magnetic field and solve the ALP-photon mixing equation [58] to find the oscillation probability in the region of interest (ROI) in the sky. We use the gammaALPS package [59] to calculate the oscillation probability in the Galactic magnetic field in different directions of the sky, $P_{a\gamma}(\ell, b)$, for given values of E_a, m_a, $g_{a\gamma\gamma}$, and take the average as

$$\langle P \rangle_{a\gamma} = \frac{4}{4\Delta\Omega} \int_0^\pi d\ell \int_{b_{\min}}^{b_{\max}} db \cos b \, P_{a\gamma}(\ell, b), \quad (11)$$

where $\Delta\Omega = \int_0^\pi d\ell \int_{b_{\min}}^{b_{\max}} db \cos b$ with ℓ and b being the galactic latitude and longitude respectively. Here we consider $b_{\min} = 5°$ and $b_{\max} = 10°$ in order to exclude the Galactic Center region.

Using Eqs. (10) and (11), the gamma-ray flux arising due to the oscillation of DSALPB ALPs into photons while passing through the galactic magnetic field can be obtained as

---

[4]Since we consider light ALPs ($m_a \lesssim 10^{-11}$ eV), the dominant photon production channel is oscillation while the decay to two photons is suppressed.
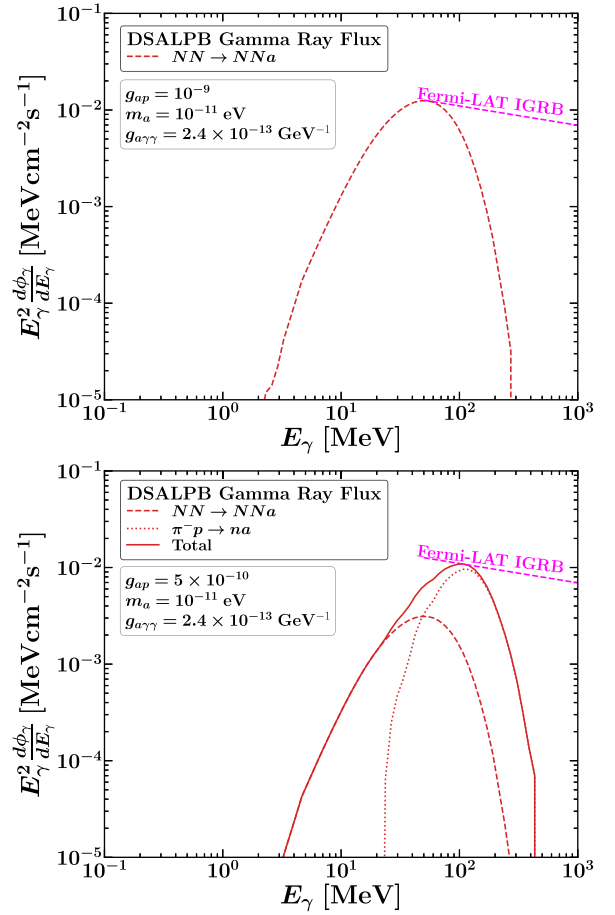

FIG. 3. Diffuse photon flux as a function of photon energy. In the upper panel, we consider ALP production only via bremsstrahlung (red dashed line) and $g_{ap} = 10^{-9}$. In the lower panel, ALP production via bremsstrahlung (red dashed line), pion conversion (red dotted line) have been considered for $g_{ap} = 5 \times 10^{-10}$ and the total flux is denoted by solid red line. In both panels, the magenta line denotes the IGRB flux measured by *Fermi*-LAT. We fix $m_a = 10^{-11}$ eV and $g_{a\gamma\gamma} = 2.4 \times 10^{-13}$ GeV^{-1} in both panels.

$$\frac{d\phi_\gamma}{dE_\gamma} = \frac{d\phi_a}{dE_a} \langle P \rangle_{a\gamma}. \quad (12)$$

In Fig. 3, we show the diffuse photon flux as a function of photon energy and compare it with the isotropic gamma-ray background (IGRB) flux measured by *Fermi*-LAT which is well-fitted by [43,60]

$$\Phi(E_\gamma) = 4\pi \times 2.2 \times 10^{-3} \left(\frac{E_\gamma}{1 \text{ MeV}} \right)^{-2.2} \text{ MeV}^{-1} \text{ cm}^{-2} \text{ s}^{-1}. \quad (13)$$

In the upper panel, we consider ALP production via bremsstrahlung only and fix $g_{ap} = 10^{-9}$, corresponding to the maximum value of g_{ap} allowed by SN 1987A cooling
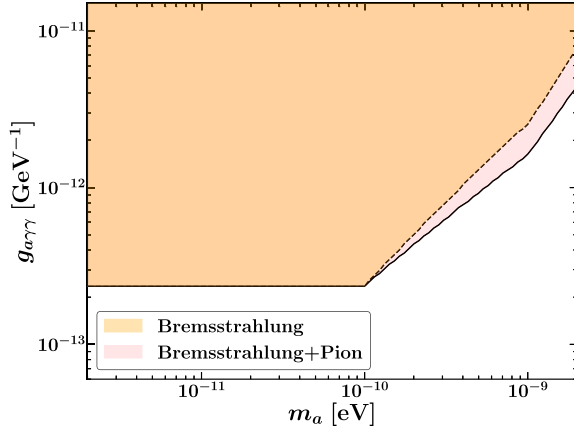
FIG. 4. Constraints in $m_a - g_{a\gamma\gamma}$ plane from *Fermi*-LAT considering supernova ALP production via NN-bremsstrahlung only (orange shaded region) and NN-bremsstrahlung + pion conversion (pink shaded region). For deriving the constraint for the bremsstrahlung only case, we have assumed $g_{ap} = 10^{-9}$ whereas for the case considering both pion and bremsstrahlung we have assumed $g_{ap} = 5 \times 10^{-10}$. These are the values that saturate the respective SN cooling bounds.

argument in the case of ALP emission via bremsstrahlung [21]. In the lower panel, we consider the ALP production via bremsstrahlung as well as pion conversion for $g_{ap} = 5 \times 10^{-10}$, the upper limit on g_{ap} from SN 1987A cooling in the presence of negatively charged pions in SN core [21]. In this case, the cooling bound is stronger by a factor of 2 due to an extra ALP production channel. As a result, the ALP flux produced by bremsstrahlung is reduced by a factor of 4. In spite of this, as shown in Fig. 4, the ALP parameter space constrained by the *Fermi*-LAT observations is not reduced since the ALPs produced from the pionic processes show a harder spectrum compared to the ALPs produced from bremsstrahlung and the *Fermi*-LAT effective area increases significantly at higher energies.

V. LIMITS AND PROJECTION ON THE ALP-PHOTON COUPLING FROM DSNALPB

In this section, we review the ALP bound from *Fermi*-LAT and estimate the sensitivity of proposed future missions. Let us start from *Fermi*-LAT. In Fig. 4, we show the limit on $g_{a\gamma\gamma}$ considering ALP production from NN-bremsstrahlung and pion-conversion for $g_{ap} = 5 \times 10^{-10}$. For comparison, we also show the limit on $g_{a\gamma\gamma}$ considering ALP production only from NN-bremsstrahlung for $g_{ap} = 10^{-9}$. For $m_a \ll 10^{-10}$ eV both of these constraints are comparable since the ALP-photon oscillation probability does not depend on the photon energy. However, for $m_a > 10^{-10}$ eV, the ALP-photon oscillation probability increases with the photon energy. In this case, we highlight that the bound in the case of bremsstrahlung + pion processes is more constraining at higher masses than the

TABLE I. List of future experiments and their specifications used in our analysis.

Experiment	Energy range [MeV]	N_{Bkg} [cts s^{-1}]
AMEGO-X [45]	50–200	1.36
e-ASTROGAM [46]	50–200	13.38
MAST [48]	50–200	18.31
GRAMS-satellite [47]	10–100	1031.25
GRAMS-balloon [47]	10–100	390.98

bremsstrahlung only case. This is not surprising since the ALPs produced from negatively charged pions have a harder spectrum and the ALP-photon oscillations are kept coherent up to larger masses at higher energies.

To derive the constraints from future telescopes, first we calculate the total number of background events within the energy range $E_{\min} \leq E_\gamma \leq E_{\max}$ as [61]

$$N_{\text{Bkg}} = 4\pi \int_{E_{\min}}^{E_{\max}} \frac{d\Phi_{\gamma,\text{Bkg.}}}{dE_\gamma} A_{\text{eff}}(E_\gamma) dE_\gamma, \qquad (14)$$

where $\frac{d\Phi_{\gamma,\text{Bkg}}}{dE_\gamma}$ is the background photon flux expressed in units of ctsMeV^{-1}s^{-1} sr^{-1}, and A_{eff} is the effective area of the telescope, which is a function of the photon energy. We estimate N_{Bkg} using the data given in Ref. [46] for e-ASTROGAM, Ref. [45] for AMEGO-X, Ref. [47] for GRAMS-balloon and its upgraded version GRAMS-satellite, and Ref. [48] for MAST. The summary of the specifications of future experiments is given in Table I.

Finally, we estimate the total number of signal events using the specifications of each telescope as

$$N_{\text{Sig}} = \int_{E_{\min}}^{E_{\max}} \frac{d\phi_\gamma}{dE_\gamma} A_{\text{eff}}(E_\gamma) dE_\gamma, \qquad (15)$$

where $\frac{d\phi_\gamma}{dE_\gamma}$ is given in Eq. (12) and we impose $N_{\text{Sig}} \geq N_{\text{Bkg}}$ to derive the upper limit on $g_{a\gamma\gamma}$.

The projected limits from future gamma-ray telescopes in the $m_a - g_{a\gamma\gamma}$ plane are summarized in Fig. 1. There, the gray shaded region shows the combined constraints in this region of parameter space from spectral distortion of radio-quiet quasar H1821 + 643 by Chandra [62], NuStar observation from M82 [63], hard x-ray observation from Betelgeuse [64], x-ray observation from super star clusters [65], and Chandra observation of AGN NGC1275 at the center of Perseus cluster [66]. For the sake of clarity, all of these limits are derived by assuming ALP coupling only with photons. We find that, in the scenario in which ALPs couple also with nucleons, the constraint derived from AMEGO-X, e-ASTROGAM, GRAMS-balloon and GRAMS-satellite are not competitive with the *Fermi*-LAT constraint, and that *only* MAST has the potential to

constrain $g_{a\gamma\gamma}$ up to a few $\times\, 10^{-13}$ GeV^{-1}, comparable to the *Fermi*-LAT bound.

Finally, we also show our updated constraint from the nonobservation of ALP-induced γ-ray burst from SN 1987A. In our scenario, we consider $g_{ap} = 5 \times 10^{-10}$ and use the measurement of the γ-ray flux from SN 1987A observed by the Gamma Ray Spectrometer (GRS) on board the Solar Maximum Mission (SMM) (see [61,67] for the limits in the scenario where $g_{a\gamma\gamma}$ and g_{ap} are not independent). Following [28–30,43], we consider the distance of SN 1987A $d_{\text{SN}} = 50$ kpc, galactic latitude $(b) = -32.1°$ and longitude $((l) = -279.5°$ and calculate the fluence $(\mathcal{F})$ within[5] $E_\gamma = [25, 100]$ MeV as

$$\mathcal{F} = \frac{1}{4\pi d_{\text{SN}}^2} \int \left(\frac{dN_a}{dE_a}\right)_{E_a = E_\gamma} P_{a\gamma}(\ell, b) dE_\gamma. \quad (16)$$

We impose $\mathcal{F} \leq 0.6$ cm^{-2} to derive the upper limit on $g_{a\gamma\gamma}$ at 95% confidence level, as shown by the solid red line in Fig. 1.

Notice that the ALPs from pionic processes have energies well above the energy band $E_\gamma = [25, 100]$ MeV used to set the bound from SN 1987A [30]. Thus, these ALPs do not affect the expected event counting. This is evident from the overlapping solid red and black dotted lines in Fig. 1. In the former case, ALP production from both bremsstrahlung and pion conversion is considered, whereas in the latter, only bremsstrahlung is included. Nevertheless, the presence of pions strengthens the cooling bound, forcing the ALP coupling to protons to a lower value. As a result, the overall ALP flux is reduced and the SN 1987A constraint from the Solar Maximum Mission (SMM), as shown in Fig. 1, is slightly weaker than the bound derived in Ref. [43].

VI. DISCUSSION AND CONCLUSIONS

ALPs coupled to nucleons can be produced in the core of a SN via *NN*-bremsstrahlung as well as through pion conversion. The presence of negatively charged pions makes the emitted ALP spectrum significantly harder than that produced solely through bremsstrahlung processes. In this work, we considered ALP production from all past core-collapse SNe, which gives rise to a diffuse ALP background with characteristic energies of $\mathcal{O}(100)$ MeV. These energetic ALPs can convert into photons in the Galactic magnetic field, generating a diffuse gamma-ray background.

After recomputing this diffuse background, including the previously overlooked contribution from the processes in

SNe involving negatively charged pions, we revisited the constraints on the DSALPB using *Fermi*-LAT observations and present updated projections for future gamma-ray telescopes including AMEGO-X, e-ASTROGAM, GRAMS-balloon, GRAMS-satellite, and MAST. We find that the *Fermi*-LAT constraint on the ALP-photon coupling $g_{a\gamma\gamma}$ is improved for ALP masses $m_a \gtrsim 10^{-10}$ eV when pion conversion is included as a production channel, as *Fermi*-LAT is more sensitive to the harder spectrum predicted in this case. Furthermore, we show that MAST could probe values of $g_{a\gamma\gamma}$ up to a few $\times\, 10^{-13}$ GeV^{-1}, a value competitive with the *Fermi*-LAT constraint.

Finally, we have updated the constraint from the nonobservation of the ALP-induced gamma-ray burst associated with SN 1987A, showing that it remains approximately one order of magnitude stronger than the strongest bound we can expect from DSALPB searches. A more detailed spectral analysis over the background of the *Fermi*-LAT experiment, along the lines discussed in Ref. [35], could potentially improve the constraint on the DSALPB. Such an analysis is beyond the scope of the present work and will be addressed elsewhere.

---

[5]In our analysis, we do not consider other energy bins such as [4.1–6.4] MeV and [10–25] MeV since in these bins, ALP flux is subdominant in comparison to the flux in the energy bin [25, 100] MeV.

DATA AVAILABILITY

No data were created or analyzed in this study.

[1] G. G. Raffelt, *Stars as Laboratories for Fundamental Physics: The Astrophysics of Neutrinos, Axions, and other Weakly Interacting Particles* (University of Chicago Press, Chicago, 1996).

[2] G. G. Raffelt, Astrophysical axion bounds, Lect. Notes Phys. **741**, 51 (2008).

[3] T. Fischer, S. Chakraborty, M. Giannotti, A. Mirizzi, A. Payez, and A. Ringwald, Probing axions with the neutrino signal from the next galactic supernova, Phys. Rev. D **94**, 085012 (2016).

[4] A. Caputo and G. Raffelt, Astrophysical axion bounds: The 2024 edition, Proc. Sci. COSMICWISPers (2024) 041 [arXiv:2401.13728].

[5] P. Carenza, M. Giannotti, J. Isern, A. Mirizzi, and O. Straniero, Axion astrophysics, Phys. Rep. **1117**, 1 (2025).

[6] P. Carenza, Axion emission from supernovae: A cheatsheet, Eur. Phys. J. Plus **138**, 836 (2023).

[7] M. S. Turner, Axions from SN 1987a, Phys. Rev. Lett. **60**, 1797 (1988).

[8] A. Burrows, M. S. Turner, and R. P. Brinkmann, Axions and SN 1987a, Phys. Rev. D **39**, 1020 (1989).

[9] A. Burrows, M. T. Ressell, and M. S. Turner, Axions and SN1987A: Axion trapping, Phys. Rev. D **42**, 3297 (1990).

[10] G. Raffelt and D. Seckel, Bounds on exotic particle interactions from SN 1987a, Phys. Rev. Lett. **60**, 1793 (1988).

[11] G. G. Raffelt, Astrophysical methods to constrain axions and other novel particle phenomena, Phys. Rep. **198**, 1 (1990).

[12] W. Keil, H.-T. Janka, D. N. Schramm, G. Sigl, M. S. Turner, and J. R. Ellis, A fresh look at axions and SN-1987A, Phys. Rev. D **56**, 2419 (1997).

[13] C. Hanhart, D. R. Phillips, and S. Reddy, Neutrino and axion emissivities of neutron stars from nucleon-nucleon scattering data, Phys. Lett. B **499**, 9 (2001).

[14] M. Giannotti and F. Nesti, Nucleon-nucleon Bremsstrahlung emission of massive axions, Phys. Rev. D **72**, 063005 (2005).

[15] P. Carenza, T. Fischer, M. Giannotti, G. Guo, G. Martínez-Pinedo, and A. Mirizzi, Improved axion emissivity from a supernova via nucleon-nucleon bremsstrahlung, J. Cosmol. Astropart. Phys. 10 (2019) 016; 05 (2020) E01.

[16] K. Choi, H. J. Kim, H. Seong, and C. S. Shin, Axion emission from supernova with axion-pion-nucleon contact interaction, J. High Energy Phys. 02 (2022) 143.

[17] P. Carenza, B. Fore, M. Giannotti, A. Mirizzi, and S. Reddy, Enhanced supernova axion emission and its implications, Phys. Rev. Lett. **126**, 071102 (2021).

[18] T. Fischer, P. Carenza, B. Fore, M. Giannotti, A. Mirizzi, and S. Reddy, Observable signatures of enhanced axion emission from protoneutron stars, Phys. Rev. D **104**, 103012 (2021).

[19] A. Lella, P. Carenza, G. Lucente, M. Giannotti, and A. Mirizzi, Protoneutron stars as cosmic factories for massive axionlike particles, Phys. Rev. D **107**, 103017 (2023).

[20] S.-Y. Ho, J. Kim, P. Ko, and J.-h. Park, Supernova axion emissivity with $\Delta(1234)$ resonance in heavy baryon chiral perturbation theory, Phys. Rev. D **107**, 075002 (2023).

[21] A. Lella, P. Carenza, G. Co', G. Lucente, M. Giannotti, A. Mirizzi, and T. Rauscher, Getting the most on supernova axions, Phys. Rev. D **109**, 023001 (2024).

[22] A. Ayala, I. Domínguez, M. Giannotti, A. Mirizzi, and O. Straniero, Revisiting the bound on axion-photon coupling from globular clusters, Phys. Rev. Lett. **113**, 191302 (2014).

[23] O. Straniero, A. Ayala, M. Giannotti, A. Mirizzi, and I. Dominguez, Axion-photon coupling: Astrophysical constraints, in *Proceedings of the 11th Patras Workshop on Axions, WIMPs and WISPs* (2015), pp. 77–81, https://bib-pubdb1.desy.de/record/316736.

[24] M. J. Dolan, F. J. Hiskens, and R. R. Volkas, Advancing globular cluster constraints on the axion-photon coupling, J. Cosmol. Astropart. Phys. 10 (2022) 096.

[25] D. Cadamuro and J. Redondo, Cosmological bounds on pseudo Nambu-Goldstone bosons, J. Cosmol. Astropart. Phys. 02 (2012) 032.

[26] P. Carenza, O. Straniero, B. Döbrich, M. Giannotti, G. Lucente, and A. Mirizzi, Constraints on the coupling with photons of heavy axion-like-particles from globular clusters, Phys. Lett. B **809**, 135709 (2020).

[27] G. Lucente, O. Straniero, P. Carenza, M. Giannotti, and A. Mirizzi, Constraining heavy axionlike particles by energy deposition in globular cluster stars, Phys. Rev. Lett. **129**, 011101 (2022).

[28] J. A. Grifols, E. Masso, and R. Toldra, Gamma-rays from SN1987A due to pseudoscalar conversion, Phys. Rev. Lett. **77**, 2372 (1996).

[29] J. W. Brockway, E. D. Carlson, and G. G. Raffelt, SN1987A gamma-ray limits on the conversion of pseudoscalars, Phys. Lett. B **383**, 439 (1996).

[30] A. Payez, C. Evoli, T. Fischer, M. Giannotti, A. Mirizzi, and A. Ringwald, Revisiting the SN1987A gamma-ray limit on

ultralight axion-like particles, J. Cosmol. Astropart. Phys. 02 (2015) 006.

[31] S. Hoof and L. Schulz, Updated constraints on axion-like particles from temporal information in supernova SN1987A gamma-ray data, J. Cosmol. Astropart. Phys. 03 (2023) 054.

[32] M. Meyer and T. Petrushevska, Search for axionlike-particle-induced prompt γ-ray emission from extragalactic core-collapse supernovae with the *Fermi* large area telescope, Phys. Rev. Lett. **124**, 231101 (2020); **125**, 119901(E) (2020).

[33] F. Calore, P. Carenza, C. Eckner, T. Fischer, M. Giannotti, J. Jaeckel, K. Kotake, T. Kuroda, A. Mirizzi, and F. Sivo, 3D template-based Fermi-LAT constraints on the diffuse supernova axion-like particle background, Phys. Rev. D **105**, 063028 (2022).

[34] F. Calore, P. Carenza, C. Eckner, M. Giannotti, G. Lucente, A. Mirizzi, and F. Sivo, Uncovering axionlike particles in supernova gamma-ray spectra, Phys. Rev. D **109**, 043010 (2024).

[35] A. Lella, F. Calore, P. Carenza, C. Eckner, M. Giannotti, G. Lucente, and A. Mirizzi, Probing protoneutron stars with gamma-ray axionscopes, J. Cosmol. Astropart. Phys. 11 (2024) 009.

[36] P. Carenza, G. Co, M. Giannotti, A. Lella, G. Lucente, A. Mirizzi, and T. Rauscher, Cross section for supernova axion observation in neutrino water Čherenkov detectors, Phys. Rev. C **109**, 015501 (2024).

[37] S. Asai, Y. Kanazawa, T. Moroi, and T. Sichanugrist, Observing axion emission from supernova with collider detectors, Phys. Lett. B **829**, 137137 (2022).

[38] F. Arias-Aragón, M. Giannotti, G. G. di Cortona, and F. Mescia, Axion-induced pair production: A new strategy for axion detection, Phys. Rev. D **111**, 043021 (2025).

[39] S.-F. Ge, K. Hamaguchi, K. Ichimura, K. Ishidoshiro, Y. Kanazawa, Y. Kishimoto, N. Nagata, and J. Zheng, Supernova-scope for the Direct Search of Supernova Axions, J. Cosmol. Astropart. Phys. 11 (2020) 059.

[40] C.-C. Li, T.-R. Hu, F.-K. Guo, and U.-G. Meißner, Pion axioproduction revisited, Phys. Rev. D **109**, 075050 (2024).

[41] P. Carenza, J. A. García Pascual, M. Giannotti, I. G. Irastorza, M. Kaltschmidt, A. Lella, A. Lindner, G. Lucente, A. Mirizzi, and M. J. Puyuelo, Detecting supernova axions with IAXO, arXiv:2502.19476.

[42] D. Alonso-González, D. Cerdeño, M. Cermeño, and A. D. Perez, Probing a diffuse flux of axion-like particles from galactic supernovae with neutrino water Cherenkov detectors, Phys. Rev. D **111**, 083019 (2025).

[43] F. Calore, P. Carenza, M. Giannotti, J. Jaeckel, and A. Mirizzi, Bounds on axionlike particles from the diffuse supernova flux, Phys. Rev. D **102**, 123005 (2020).

[44] J. N. Benabou, C. A. Manzari, Y. Park, G. Prabhakar, B. R. Safdi, and I. Savoray, Time-delayed gamma-ray signatures of heavy axions from core-collapse supernovae, Phys. Rev. D **111**, 095029 (2025).

[45] R. Caputo *et al.*, All-sky medium energy gamma-ray observatory eXplorer mission concept, J. Astron. Telesc. Instrum. Syst. **8**, 044003 (2022).

[46] A. De Angelis *et al.* (e-ASTROGAM Collaboration), The e-ASTROGAM mission, Exp. Astron. **44**, 25 (2017).

[47] T. Aramaki, P. Hansson Adrian, G. Karagiorgi, and H. Odaka, Dual MeV gamma-ray and dark matter observatory-GRAMS project, Astropart. Phys. **114**, 107 (2020).

[48] T. Dzhatdoev and E. Podlesnyi, Massive Argon Space Telescope (MAST): A concept of heavy time projection chamber for γ-ray astronomy in the 100 MeV–1 TeV energy range, Astropart. Phys. **112**, 1 (2019).

[49] C. O'Hare, cajohare/axionlimits: Axionlimits, https://cajohare.github.io/AxionLimits/ (2020).

[50] L. Di Luzio, M. Giannotti, E. Nardi, and L. Visinelli, The landscape of QCD axion models, Phys. Rep. **870**, 1 (2020).

[51] R. P. Brinkmann and M. S. Turner, Numerical rates for nucleon-nucleon axion Bremsstrahlung, Phys. Rev. D **38**, 2338 (1988).

[52] B. Fore and S. Reddy, Pions in hot dense matter and their astrophysical implications, Phys. Rev. C **101**, 035809 (2020).

[53] Garching core-collapse supernova research archive, https://wwwmpa.mpa-garching.mpg.de/ccsnarchive//.

[54] A. Lella, E. Ravensburg, P. Carenza, and M. C. D. Marsh, Supernova limits on QCD axionlike particles, Phys. Rev. D **110**, 043019 (2024).

[55] G. Grilli di Cortona, E. Hardy, J. Pardo Vega, and G. Villadoro, The QCD axion precisely, J. High Energy Phys. 01 (2016) 034.

[56] J. Eby and V. Takhistov, Diffuse axion background, arXiv:2402.00100.

[57] A. Priya and C. Lunardini, Diffuse neutrinos from luminous and dark supernovae: prospects for upcoming detectors at the $O(10)$ kt scale, J. Cosmol. Astropart. Phys. 11 (2017) 031.

[58] G. Raffelt and L. Stodolsky, Mixing of the photon with low mass particles, Phys. Rev. D **37**, 1237 (1988).

[59] M. Meyer, J. Davies, and J. Kuhlmann, gammaALPS: An open-source Python package for computing photon-axion-like-particle oscillations in astrophysical environments, Proc. Sci. ICRC2021 (**2021**) 557 [arXiv:2108.02061].

[60] Fermi Gamma-ray Telescope, https://fermi.gsfc.nasa.gov/ssc/data/access/lat/BackgroundModels.html.

[61] F. Lecce, A. Lella, G. Lucente, V. Vijayan, A. Bauswein, M. Giannotti, and A. Mirizzi, Probing axion-like particles with multimessenger observations of neutron star mergers, arXiv:2504.02032.

[62] J. S. Reynés, J. H. Matthews, C. S. Reynolds, H. R. Russell, R. N. Smith, and M. C. D. Marsh, New constraints on light axion-like particles using Chandra transmission grating spectroscopy of the powerful cluster-hosted quasar H1821 + 643, Mon. Not. R. Astron. Soc. **510**, 1264 (2021).

[63] O. Ning and B. R. Safdi, Leading Axion-photon sensitivity with NuSTAR observations of M82 and M87, Phys. Rev. Lett. **134**, 171003 (2025).

[64] M. Xiao, K. M. Perez, M. Giannotti, O. Straniero, A. Mirizzi, B. W. Grefenstette, B. M. Roach, and M. Nynka, Constraints on axionlike particles from a hard x-ray observation of betelgeuse, Phys. Rev. Lett. **126**, 031101 (2021).

[65] C. Dessert, J. W. Foster, and B. R. Safdi, X-ray searches for axions from super star clusters, Phys. Rev. Lett. **125**, 261102 (2020).

[66] C. S. Reynolds, M. C. D. Marsh, H. R. Russell, A. C. Fabian, R. Smith, F. Tombesi, and S. Veilleux, Astrophysical limits on very light axion-like particles from Chandra grating spectroscopy of NGC 1275, Astrophys. J. **890**, 59 (2020).

[67] C. A. Manzari, Y. Park, B. R. Safdi, and I. Savoray, Supernova axions convert to gamma rays in magnetic fields of progenitor stars, Phys. Rev. Lett. **133**, 211002 (2024).